



Fluid flow modeling of resin transfer molding for composite material wind turbine blade structures by Scott Montgomery Rossell

A thesis submitted in partial fulfillment of the requirements for the degree Of Master of Science in
Chemical Engineering

Montana State University

© Copyright by Scott Montgomery Rossell (2000)

Abstract:

Resin transfer molding (RTM) is a closed mold process for making composite materials. It has the potential to produce parts more cost effectively than hand lay-up or other methods. However, fluid flow tends to be unpredictable and parts the size of a wind turbine blade are difficult to engineer RTM without some predictive method for resin flow.

There were five goals of this study. The first was to determine permeabilities for three fabrics commonly used for RTM over a useful range of fiber volume fractions. Next, relations to estimate permeabilities in mixed fabric lay-ups were evaluated. Flow in blade substructures was to be analyzed and compared to predictions. Flow in a full-scale blade was to be predicted and substructure results were to be used to validate the accuracy of a full-scale blade prediction.

Permeabilities were calculated for three fabrics (A130, DB120 and D155) in the fiber volume fraction range of 0.27 to 0.47. In addition, relations were determined for each fabric over the given range of fiber volume fractions.

Two estimation methods were used to predict flow. One method was based on the relative thickness of glass in the fabrics and the other was based on the thickness of fabric layers at a given clamping pressure.. The clamping pressure method was able to accurately predict the flow front shapes of a lay-up, but tended to under predict permeabilities. The relative thickness method did not capture the proper flow front shapes and under predicted permeabilities as well.

Liquid Injection Modeling Simulation LIMS was used to predict flow in the substructural models. Substructures in which flow was analyzed include a thick flanged T-section and a steel root insert. Filling times were well predicted in the T-section, but flow front shapes were not exact due to preferential flow in the mold. The steel root insert section was not well predicted due to the complex lay-up and a significant amount of interlaminar flow.

Two full blade simulations were created. One was an end injection and the other consisted of 6 injection ports in three stations. Ports were located at the flange on the low and high pressure sides of the blade at each station. Filling times were reduced by a factor of 10 using the 3 stage injection instead of injection from an end.

Based on results from the substructure experiments, the blade filling times are over predicted. Due to the large scale of the blade, interlaminar flow problems should be negligible so flow front shapes should be accurately predicted.

FLUID FLOW MODELING OF RESIN TRANSFER MOLDING FOR COMPOSITE
MATERIAL WIND TURBINE BLADE STRUCTURES

by

Scott Montgomery Rossell

A thesis submitted in partial fulfillment
of the requirements for the degree

of

Master of Science

in

Chemical Engineering

MONTANA STATE UNIVERSITY-BOZEMAN
Bozeman, Montana

August, 2000

N 318

R 7349

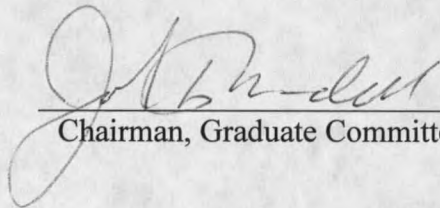
APPROVAL

of a thesis submitted by

Scott Montgomery Rossell

This thesis has been read by each member of the thesis committee and has been found to be satisfactory regarding content, English usage, format, citations, bibliographic style, and consistency, and is ready for submission to the College of Graduate Studies.

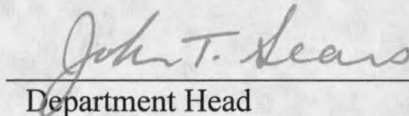
Dr. John F. Mandell


Chairman, Graduate Committee

8/8/00
Date

Approved for the Department of Chemical Engineering

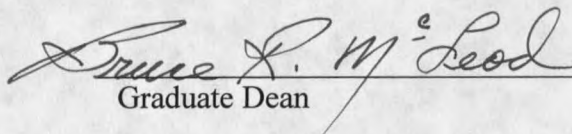
Dr. John T. Sears


Department Head

8/11/00
Date

Approved for the College of Graduate Studies

Dr. Bruce McLeod


Graduate Dean

9-1-00
Date

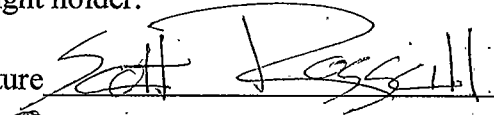
STATEMENT OF PERMISSION TO USE

In presenting this thesis in partial fulfillment of the requirements for a master's degree at Montana State University-Bozeman, I agree that the Library shall make it available to borrowers under rules of the Library.

If I have indicated my intention to copyright this thesis by including a copyright notice page, copying is allowable only for scholarly purposes, consistent with "fair use" as prescribed in the U.S. Copyright Law. Requests for permission for extended quotation from or reproduction of this thesis in whole or in parts may be granted only by the copyright holder.

Signature

Date

8-14-00

ACKNOWLEDGMENTS

First and foremost I would like to thank my parents and Ashley for their encouragement and patience through out this process. Without your support I'm not sure I would have been able to keep my sanity.

This project would not have been possible with out the guidance and direction provided by my advisors: Dr. Mandell, Dr. Cairns and Dr. Larsen. I would also like to thank Daniel Samborsky for all his help and procuring the necessary equipment for the project. Aaron Cook and Russell Evertz also deserve recognition. Aaron provided a camera when mine was broken and helped with the testing and data acquisition for the fabric compression tests. Russ's help with gathering relative thickness data also deserves thanks. At one point in time I have received advice or assistance from all the members of the MSU Composites Group. I would like to thank all of you for making my stay here an enjoying and memorable one.

TABLE OF CONTENTS

LIST OF FIGURES	ix
LIST OF TABLES	xiii
ABSTRACT	xvi
1 INTRODUCTION	1
Motivation	2
Objective and Approach	5
Organization of Thesis	6
2 BACKGROUND	7
Composite Materials	7
Material Properties	8
Resin Systems	9
Fiber Reinforcements	9
Composite Manufacturing	10
Hand Lay-up	11
RTM	12
Flow Theory	13
Preform Geometry	14
General Flow	16
Darcy's Law	16
Permeability Determination	18
Numerical Calculation Methods	19
Experimental Calculation Methods	21
Sources of Error	24
Modeling Theory	25
Micro Modeling Schemes	26
MSU Micro Model	26
Macro-Flow Modeling Schemes	27
LIMS	28
Flow Phenomena (Sources for Modeling Error)	29
3 EXPERIMENTAL METHODS AND PROCEDURES	31
Materials and Process Equipment	31
E-glass fiber reinforcement	31
Resin System	34
Injection Equipment	35
Molds	36

Flat plate mold.....	36
Thick Flanged T-section Mold	37
Steel Root Insert Mold	39
Imaging Equipment.....	40
Resin and Fabric Characterization.....	40
Motivation	40
Resin Viscosity.....	41
Surface tension	43
Capillary Pressure	44
Experiment Designation Scheme.....	44
Fiber Volume Fraction.....	45
Fiber Stacking and Compressibility.....	46
Permeability	49
Motivation and Test Matrix	49
Experimental Methods	49
Mixed Fabric	52
Motivation and Test Matrix	52
Predictive Methods	53
Experimental Procedures	54
T-Section	54
Motivation and Test Matrix	54
Experimental Methods.....	56
Root Insert Section.....	57
Experimental Procedures	58
4 EXPERIMENTAL RESULTS	60
Resin and Fabric Characterization.....	60
Viscosity.....	60
Surface Tension.....	63
Capillary Pressure	64
Fiber Volume Fraction.....	65
Fabric Stacking and Compressibility.....	66
Permeability	72
A130 Fabric.....	73
DB120 Fabric Results	75
D155 Fabric.....	77
Permeability Discussion	79
Mixed Fabric	84
Experimental Results	84
Predictive Data used.....	87
Predictive Results.....	88
Summary	97
T-Section	98
TA01.....	98

TD01.....	101
TA02.....	103
Steel Root Insert Mold.....	105
5 NUMERICAL RESULTS AND CORRELATION WITH EXPERIMENTS.....	107
LIMS basics	107
Model Creation.....	107
LIMS input parameters	110
Recording information	111
Flat Plate models.....	111
Experimental Error.....	112
A130 0 ₈ Lay-up (SA08-1).....	112
D155 0 ₆ Lay-up (SD06-1).....	114
A130-DB120 [0/±45 ₂ /0]s Lay-up.....	115
A130 [0/90/0/90]s Lay-up	116
T-section Results.....	118
Thick flanged T model.....	118
A130 Center Injected T-mold (TA01).....	119
D155 Center Injected T-mold (TD01).....	121
A130 End Injected T-mold (TA02).....	123
Steel Insert Results.....	125
Insert Model	126
Results	128
Blade Models	129
Model.....	130
End Injection	130
Multiple Port injection	131
Discussion	133
6 RESULTS SUMMARY, RECOMMENDATIONS AND FUTURE WORK.....	134
Fabric Characterization.....	134
Permeability	135
Single Fabric Permeability.....	135
Mixed Fabric Permeability	135
Modeling	136
Thick Flange T Mold	136
Steel Insert Mold.....	136
Blade.....	137
Recommendations.....	137
Future Work	138
REFERENCES CITED	139
APPENDICES	143

APPENDIX A	144
Description of Calculations	145
Mixed Fabric Experiments.....	153
APPENDIX B	160
Relative Thickness Example Calculation.....	161
Clamping Pressure Example Calculation	161
APPENDIX C	163
Key-points along Blade.....	164
Lay-up Information and Permeabilities for Blade Model.....	165

LIST OF FIGURES

Figure 1. AOC 15/50 blade and cross section (length is approximately 8 m).	2
Figure 2. Components of the AOC 15/50:	3
Figure 3. Rough inside surface of a wind turbine blade.	3
Figure 4. Thick bond line in a wind turbine blade	4
Figure 5. Cross section of a $[0/90_2/0]$ composite.	7
Figure 6. Schematic of the axis relative to a roll of fabric.....	10
Figure 7. Diagram of a simple RTM injection setup.	12
Figure 8. Multiple length scales for flow.	14
Figure 9. Common fabrics used for RTM and hand lay-up.....	15
Figure 10. D155 fiber bundle.	15
Figure 11. Generalized flow for an anisotropic medium with an injection port of radius R_0 centered at $(0,0)$	22
Figure 12. Stacking sequence for a $[+45/0/-45]$ lay-up. Fibers are the solid regions and channels are void spaces between fibers.....	27
Figure 13. Photograph showing a void area in a T-section.	29
Figure 14. Three regions of flow in an RTM mold.....	30
Figure 15. A130 Fabric.....	32
Figure 16. D155 Fabric.....	33
Figure 17. DB120 Fabric	34
Figure 18. 0° and $\pm 45^\circ$ sides of CDB200 fabric.	34
Figure 19. Pressure pot.	36
Figure 20. Flat plate mold.....	37
Figure 21. Schematic of thick flanged T section and its dimensions.	38

Figure 22. T-section mold.	38
Figure 23. Skin and inner-surface halves of the steel insert mold.....	40
Figure 24. Capillary rheometer.....	41
Figure 25. Fabric compression diagram.....	48
Figure 26. Diagram of experimental permeability setup.....	51
Figure 27. Regions of the AOC 15/50 that may be modeled by a flat plate geometry.	52
Figure 28. T-section part and how it relates to the AOC 15/50.....	55
Figure 29. Port locations on the thick flanged T-mold.....	55
Figure 30. Steel insert part and how it relates to the AOC 15/50.....	57
Figure 31. Lay-up of the skin side of the insert mold.....	58
Figure 32. Viscosity of catalyzed CoRezyn 63-AX-051 with time. The average value for the uncatalyzed resin is shown at time equal to 0.....	63
Figure 33. Comparison of relative thickness method prediction with experimental burn-off results.	66
Figure 34. Displacement of fabric compression test fixture without fabric as a function of load. Error bars are placed on Run 3.	67
Figure 35. Compressibility of unidirectional A130, DB120 and D155 fabrics.	69
Figure 36. Effects of lay-up on A130 fabric stacking.....	70
Figure 37. Effects of lay-up on D155 fabric stacking.....	71
Figure 38. Effect of mixed fabrics on fiber volume fraction.....	72
Figure 39. Contour plot for experiment SA08-1. Times are listed in minute_second format on the legend. The lay-up consisted of 8 layers of A130 fabric with a fiber volume fraction of 0.40.	74
Figure 40. A130 unidirectional permeability versus fiber volume fraction.....	74
Figure 41. Contour plot for experiment SB08-1. Times are listed in minute_second format on the legend. The lay-up consisted of 8 layers of DB120 fabric with a fiber volume fraction of 0.31.	76

Figure 42. Permeability versus fiber volume fraction for DB120 fabric.	77
Figure 43. Contour plot for experiment SD06-1. Times are listed in minute_second format on the legend. The lay-up consisted of 6 layers of D155 fabric with a fiber volume fraction of 0.40.	78
Figure 44. D155 permeability versus fiber volume fraction for a unidirectional lay-up.	79
Figure 45. Unsaturated flow occurring in a unidirectional A130 lay-up.	80
Figure 46. Permeability variation for three experiments with A130 fabrics.	80
Figure 47. Summary of single fabric permeability data.	81
Figure 48. Transverse and longitudinal permeabilities for mixed fabric experiments.	87
Figure 49. Plot of experimental and predicted flow fronts for test MA01-2 at 1800 sec. with an injection pressure of 86.2 kPa.	89
Figure 50. Plot of experimental and predicted flow front positions for test MD01- 1 at 500 sec. with an injection pressure of 89.7 kPa.	90
Figure 51. Summary of longitudinal permeability estimates versus experimentally determined permeabilities for the Mx01, Mx02 and Mx03 series lay-ups.	92
Figure 52. Summary of transverse permeability predictions versus experimentally determined permeabilities for the Mx01, Mx02 and Mx03 series lay-ups.	93
Figure 53. Predicted versus experimental K_x values for the Mx04 and Mx05 lay-ups.	95
Figure 54. Predicted versus experimental K_y values for the Mx04 and Mx05 lay-ups.	96
Figure 55. Source of high permeability in T-sections.	100
Figure 56. Flow front positions for TA01. Injection was from two central injection ports (shown as black dots) at a pressure of 82.7 kPa.	101
Figure 57. Flow front positions TD01. Injection was from two central injection ports (shown as black dots) at a pressure of 82.7 kPa.	103

Figure 58. Flow front positions for TA02. Injection was from two injection ports located at the end of the mold. Injection pressure was at 82.7 kPa.	104
Figure 59. Filling pattern of insert mold with an injection pressure of 96.5 kPa.....	106
Figure 60. Experimental versus predicted flow front positions for SA08-1, single fabric A130. $K_x=9.90 \times 10^{-11}$ $K_y=3.47 \times 10^{-11}$, $v_f=0.400$, $\mu=0.195$ kg/m-s and $P=89.7$ kPa.....	113
Figure 61. Experimental versus predicted results for SD08-1, single fabric D155. $K_x=2.41 \times 10^{-10}$ $K_y=1.40 \times 10^{-11}$, $v_f=0.456$, $\mu=0.195$ kg/m-s and $P=89.7$ kPa.	115
Figure 62. Flow contours comparing the experimentally determined permeability with two predictive methods. Flow front times are at 85 and 1800s from an injection port located at the origin. Quarter symmetry was assumed.	116
Figure 63. Flow contours comparing the experimentally determined permeability with the relative thickness predictive method for the MA03-2 lay-up (0/90/0/90)s. Flow front times were at 54 s, 320s and 900 s from an injection port located at the origin. Quarter symmetry was assumed.	117
Figure 64. Meshed T-mold showing the three different lay-up regions.....	119
Figure 65. Predicted versus experimental results for case TA01.	121
Figure 66. Predicted versus experimental results for case TA01.	123
Figure 67. Experimental versus predicted results for TA02.....	125
Figure 68. Sections of insert model.....	126
Figure 69. Meshed insert model with a close up at the insert tip region.....	127
Figure 70. Insert Model versus experimental results. Injection at 96.5 kPa.	129
Figure 71. Tip end of AOC 15/50 blade.....	130
Figure 72. End injection of AOC 15/50 blade. View is from the low pressure side of the blade.....	131
Figure 73. Multi-port injection of AOC 15/50 blade. Six injection ports were located at three locations along the blade length on both the low and high-pressure sides of the blade at the web skin intersection. View is from the low-pressure side of the blade.....	132

LIST OF TABLES

Table 1. Tensile properties of aluminum, E-glass, polyester resin, and E-glass, polyester composites.	8
Table 2. Summary of E-glass fabric reinforcement material used.	31
Table 3. Rheometer dimensions.	41
Table 4. Viscosity Experiments.	43
Table 5. Burn off tests.	45
Table 6. Fabric stacking and compression test matrix.	47
Table 7. Permeability test matrix.	49
Table 8. Mixed fabric test matrix.	53
Table 9. Properties of T-section components.	56
Table 10. Viscosity Results.	61
Table 11. Surface tension results.	64
Table 12. Capillary pressure.	65
Table 13. Relative thickness and fabric composition results. Results are an average of three tests performed on each fabric type.	65
Table 14. Correlations for permeability as a function of fiber volume.	88
Table 15. Ply thickness versus clamping pressure relationships.	88
Table 16. Predicted lay-up composition and permeabilities for Mx04 and Mx05 lay-ups.	94
Table 17. Comparison of predicted to experimental flow front shapes.	97
Table 18. Matrix of mesh sensitivity runs on a 510 mm by 810 mm plate model with quarter symmetry and the injection port located at the origin.	108
Table 19. Mesh sensitivity flow results.	109
Table 20. LIMS input parameters.	110

Table 21. Fabric related LIMS input properties for thick flanged T model TA01. Injection took place at 82.7 kPa from a central injection port and with a resin viscosity of 0.195 kg/m·s.....	120
Table 22. Fabric related LIMS input properties for thick flanged T model TD01. Injection took place at 82.7 kPa from a central injection port and with a resin viscosity of 0.195 kg/m·s.....	122
Table 23. Fabric related LIMS input properties for thick flanged T model TA02. Injection took place at 82.7 kPa from an end of the skin. A resin viscosity of 0.195 kg/m·s was used.....	124
Table 24. Fabric related LIMS input properties for steel insert model. Injection took place at 96.5 kPa with a resin viscosity of 0.195 kg/m·s.	127
Table 25. Example of a permeability spread sheet.	146
Table 26. Experiment SA06-1, A130 0 ₆	146
Table 27. Experiment SA07-1, A130 0 ₇	147
Table 28. Experiment SA08-1, A130 0 ₈	147
Table 29. Experiment SA08-2, A130 0 ₈	148
Table 30. Experiment SA08-3, A130 0 ₈	148
Table 31. Experiment SA09-1, A130 0 ₉	149
Table 32. Experiment SB07-1, DB120 0 ₇	149
Table 33. Experiment SB08-1, DB120 0 ₈	150
Table 34. Experiment SB10-1, DB120 0 ₁₀	150
Table 35. Experiment SB12-1, DB120 0 ₁₂	151
Table 36. Experiment SD05-1, D155 0 ₅	151
Table 37. Experiment SD06-1, D155 0 ₆	152
Table 38. Experiment SD08-1, D155 0 ₈	152
Table 39. Experiment SD09-1, D155 0 ₉	153
Table 40. Experiment MA01-1, A130 [0/90 ₂ /0]s	153

Table 41. Experiment MA01-2, A130 [0/90 ₂ /0]s	154
Table 42. Experiment MA02-1, A130 [(90/0) ₂]s.....	154
Table 43. Experiment MA03-1, A130 [0/90/0/ $\overline{90}$]s.	155
Table 44. Experiment MA03-2, A130 [0/90/0/ $\overline{90}$]s.	155
Table 45. Experiment MA04-1, A130/DB120 [0/ \pm 45/0]s.....	156
Table 46. Experiment MA05-1, A130/DB120 [0/ \pm 45/90]s.....	156
Table 47. Experiment MD01-1, D155 [0/90 ₂ /0]s.	157
Table 48. Experiment MD02-1, D155 [(90/0) ₂]s.....	157
Table 49. Experiment MD03-2, D155 [0/90/0/ $\overline{90}$]s.	158
Table 50. Experiment MD04-1, D155/DB120 [0/ \pm 45 ₂ /0]s.	158
Table 51. Experiment MD04-1, D155/DB120 [0/ \pm 45 ₂ /90]s.	159
Table 52. Key-points for blade model.....	164
Table 53. Permeabilities along blade section.....	165

ABSTRACT

Resin transfer molding (RTM) is a closed mold process for making composite materials. It has the potential to produce parts more cost effectively than hand lay-up or other methods. However, fluid flow tends to be unpredictable and parts the size of a wind turbine blade are difficult to engineer RTM without some predictive method for resin flow.

There were five goals of this study. The first was to determine permeabilities for three fabrics commonly used for RTM over a useful range of fiber volume fractions. Next, relations to estimate permeabilities in mixed fabric lay-ups were evaluated. Flow in blade substructures was to be analyzed and compared to predictions. Flow in a full-scale blade was to be predicted and substructure results were to be used to validate the accuracy of a full-scale blade prediction.

Permeabilities were calculated for three fabrics (A130, DB120 and D155) in the fiber volume fraction range of 0.27 to 0.47. In addition, relations were determined for each fabric over the given range of fiber volume fractions.

Two estimation methods were used to predict flow. One method was based on the relative thickness of glass in the fabrics and the other was based on the thickness of fabric layers at a given clamping pressure. The clamping pressure method was able to accurately predict the flow front shapes of a lay-up, but tended to under predict permeabilities. The relative thickness method did not capture the proper flow front shapes and under predicted permeabilities as well.

Liquid Injection Modeling Simulation LIMS was used to predict flow in the substructural models. Substructures in which flow was analyzed include a thick flanged T-section and a steel root insert. Filling times were well predicted in the T-section, but flow front shapes were not exact due to preferential flow in the mold. The steel root insert section was not well predicted due to the complex lay-up and a significant amount of interlaminar flow.

Two full blade simulations were created. One was an end injection and the other consisted of 6 injection ports in three stations. Ports were located at the flange on the low and high pressure sides of the blade at each station. Filling times were reduced by a factor of 10 using the 3 stage injection instead of injection from an end.

Based on results from the substructure experiments, the blade filling times are over predicted. Due to the large scale of the blade, interlaminar flow problems should be negligible so flow front shapes should be accurately predicted.

CHAPTER 1

INTRODUCTION

Advanced composite materials offer an exciting and diverse alternative to traditional materials. Their high strength and stiffness-to-weight ratios combined with a wide range of design options have allowed them to be a popular material in performance driven areas such as aerospace and sporting goods industries. In addition, they can provide a competitive, low-cost solution in piping, storage tank, and marine applications^{1,2}. Another application where advanced composites are gaining popularity is the wind industry. E-glass reinforced polyester, vinyl-ester or epoxy composites are becoming the material of choice for producing wind turbine blades. These composites allow designers to make lighter more efficient blades at an affordable price.

Wind energy is a clean, renewable source of energy. Despite the potential benefits of wind energy, its cost per kilowatt-hour remains high enough to limit its growth in the United States. One area where wind energy can see a cost reduction is in the manufacturing of wind turbine blades. Currently most composite wind turbine blades are manufactured by the hand lay-up process. The AOC 15/50 is one example³. Resin transfer molding (RTM) offers the potential of making lighter, more efficient blades while at the same time lowering production costs of the blades^{4 5}. A typical blade geometry and structure are illustrated in Figure 1³.

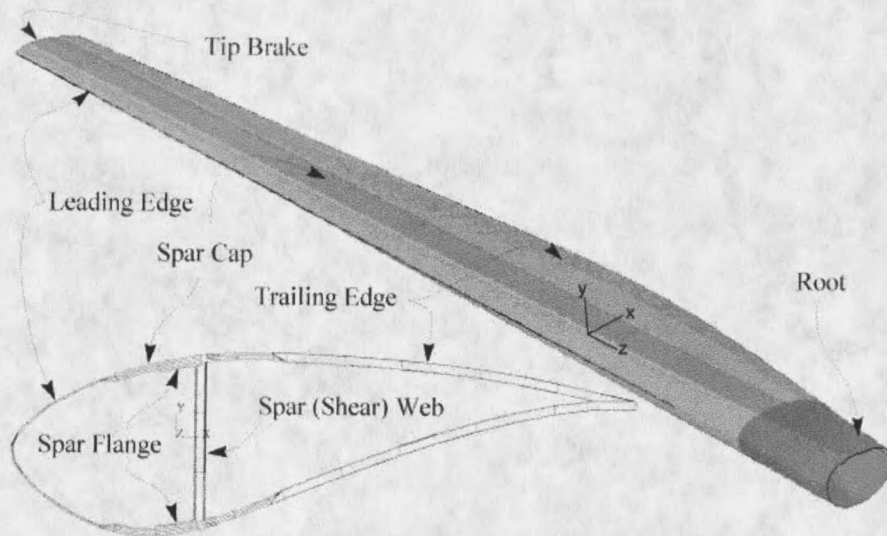


Figure 1. AOC 15/50 blade and cross section (length is approximately 8 m)³.

Motivation

Hand lay-up involves manufacturing by the sequential addition of layers of reinforcement and resin matrix in an open mold. It allows for the manufacture of a wide range of geometries and requires low initial investment. Despite these advantages, hand lay-up is not well suited to large-scale production due to the fact that it is very labor intensive and requires high cycle times. In addition, it is not possible to make hollow structures with the hand lay-up process. Therefore, a blade must be manufactured in pieces and secondary bonded together, Figure 2. The hand lay-up process uses a one-sided mold, and this adds some complications to the manufacturing process. Since there is only one mold half defining the part shape, parts tend to vary significantly in thickness and only have only one finished surface. The unfinished surface requires additional time to condition for bonding, Figure 3, and poor manufacturing tolerances may result in thick bond lines, Figure 4. Another limitation of hand lay-up, is that fiber volume fractions are

